Nanoscale Res Lett (2007) 2:365–372
DOI 10.1007/s11671-007-9077-1

NANO REVIEW

Nanomicrobiology

David Alsteens · Etienne Dague · Claire Verbelen · Guillaume Andre · Grégory Francius · Yves F. Dufrêne

Received: 24 May 2007 / Accepted: 25 June 2007 / Published online: 19 July 2007

Abstract Recent advances in atomic force microscopy (AFM) are revolutionizing our views of microbial surfaces. While AFM imaging is very useful for visualizing the surface of hydrated cells and membranes on the nanoscale, force spectroscopy enables researchers to locally probe biomolecular forces and physical properties. These unique capabilities allow us to address a number of questions that were inaccessible before, such as how does the surface architecture of microbes change as they grow or interact with drugs, and what are the molecular forces driving their interaction with antibiotics and host cells? Here, we provide a flavor of recent achievements brought by AFM imaging and single molecule force spectroscopy in microbiology.

Keywords AFM · Cells · Imaging · Force spectroscopy · Molecular recognition · Single molecule · Ultrastructure

Introduction

During the past 40 years, the importance of the microbial cell surface in biology, medicine, industry, and ecology has been increasingly recognized. Because they constitute the frontier between the cells and their environment, microbial cell walls play several key functions: supporting the internal turgor pressure of the cell, protecting the cytoplasm from the outer environment, imparting shape to the organism, acting as a molecular sieve, controlling molecular recognition and cell adhesion, and being the target of antibiotics. These functions have major consequences in biotechnology (wastewater treatment, bioremediation, and immobilized cells in reactors), industrial systems (biofouling and contamination) and medicine (interactions of pathogens with animal host tissues, accumulation on implants and prosthetic devices). This emphasizes the need to develop new techniques for probing the structure, properties and interactions of microbial surfaces.

Traditionally, probing of the cell surface architecture relies on transmission (TEM) and scanning (SEM) electron microscopy techniques [1–5]. Although cryo-methods have allowed researchers to get more natural views of bacterial cell envelopes, these approaches are very demanding in terms of sample preparation and analysis and are only applied in a few laboratories worldwide. Valuable information on the composition, properties and interactions of cell surfaces can also be gained using electron microscopy approaches, biochemical analysis, biophysical techniques and surface analysis methods [4, 5]. These techniques usually involve cell manipulation prior to examination and often provide averaged information obtained on large ensembles of cells. However, recent advances in atomic force microscopy (AFM) are helping to overcome these problems by providing three-dimensional images of hydrated cells and membranes with nanometer resolution [6, 7], and enabling researchers to probe a variety of molecular forces and physical properties on cell surfaces, including the unfolding pathways of single membrane proteins [8], the elasticity of cell walls [9], the molecular forces responsible for cell–cell and cell–solid interactions [10], and the localization of specific molecular recognition sites [11]. The number of publications in which AFM is applied to microbiological samples has increased continuously

D. Alsteens · E. Dague · C. Verbelen · G. Andre · G. Francius · Y. F. Dufrêne (✉)
Unité de Chimie des Interfaces, Université Catholique de Louvain, Croix du Sud 2/18, B-1348 Louvain-la-Neuve, Belgium
e-mail: dufrene@cifa.ucl.ac.be

over the past years, indicating that a new field is born, i.e., nanomicrobiology.

The general principle of AFM is to scan a sharp tip over the surface of a sample, while sensing the so-called near-field physical interactions between the tip and the sample. This allows three-dimensional images to be generated directly in aqueous solution. The sample is mounted on a piezoelectric scanner which ensures three-dimensional positioning with high accuracy. While the tip (or sample) is being scanned in the (x, y) directions, the force interacting between tip and specimen is monitored with piconewton sensitivity. This force is measured by the deflection of a soft cantilever which is detected by a laser beam focused on the free end of the cantilever and reflected into a photodiode.

A number of different AFM imaging modes are available, which differ mainly in the way the tip is moving over the sample. In the so-called contact mode, the AFM tip is raster scanned over the sample while the cantilever deflection, thus the force applied to the tip, is kept constant using feedback control. In dynamic or intermittent mode, an oscillating tip is scanned over the surface and the amplitude and phase of the cantilever are monitored near its resonance frequency. Because lateral forces during imaging are greatly reduced with dynamic modes, they are advantageous for imaging soft biological samples.

In force spectroscopy, the cantilever deflection is recorded as a function of the vertical displacement of the piezoelectric scanner, i.e., as the sample is pushed toward the tip and retracted. This results in a cantilever deflection versus scanner displacement curve, which can be transformed into a force-distance curve using appropriate corrections. For most microbiological applications, accurate determination of the contact point (zero separation distance) between the AFM tip and the soft sample is rather delicate due to the complex contributions of surface forces and mechanical deformation [9]. Force-distance curves can be recorded either at single, well-defined locations of the (x, y) plane or at multiple locations to yield a so-called 'force-volume image.' In doing so, spatially resolved maps of physical properties (elasticity and adhesion) and molecular interactions can be produced (for a review on force spectroscopy methodology and applications, see [12]).

Structural Imaging

Membrane Proteins

Two-dimensional crystals of membrane proteins, and more recently native membranes, have proven to be particularly well-suited for high-resolution AFM imaging and manipulation [6]. Owing to continuous progress in instrumentation, sample preparation methods and recording conditions, structural information can now be routinely obtained on membrane proteins to a resolution of 0.5–1 nm and under physiological conditions, which makes AFM a complementary tool to X-ray and electron crystallography. Examples of such protein crystalline arrays that have been visualized with subnanometer resolution include *Bacillus* S-layers [13], the hexagonally packed intermediate (HPI) layer of *Deinococcus radiodurans* [14], purple membrane from the archeon *Halobacterium* [15] and porins crystals of *Escherichia coli* [16]. Function-related conformational changes can be monitored on single proteins, as nicely demonstrated for porin OmpF in which voltage and pH-induced channel closure was observed [17]. There is also clear evidence that the instrument is evolving from an imaging technique to a multifunctional tool, enabling the measurement of multiple properties of membrane proteins [8]. In particular, the combined use of AFM imaging and single molecule force spectroscopy makes it possible to pull on single membrane proteins, thereby providing novel molecular insight into their unfolding pathways and assembly forces [18, 19].

Yet, an important bottleneck has limited the widespread use of the technique in membrane research, i.e., the need to firmly attach the specimens onto a solid support for analysis, meaning the very central concept of a native membrane separating two aqueous compartments is not preserved. One-way to circumvent this limitation is to combine AFM with patch-clamp techniques in the same experimental setup, thereby offering the exciting possibility to image non-supported membrane patches and to study currents through single ion channels [20]. More recently, a two-chamber AFM set-up was developed, by adsorbing membrane patches on holey silicon surfaces with nanoscale hole diameters and periodicities [21], enabling investigators to probe the structure, elasticity and energy of interaction of membrane proteins separating two aqueous compartments, and over which membrane gradients can be established.

Atomic force microscopy has also revealed the native ultrastructure of non-crystalline native membranes of different photosynthetic bacteria, including *Rhodopseudomonas viridis* [22], *Rhodospirillum photometricum* [23], *Rhodobacter sphaeroides* [24], *Rhodobacter blasticus* [25], and *Rhodopseudomonas palustris* [26], providing new insight on the supramolecular organization of membrane protein complexes. In one such study [23], AFM was used to investigate how the composition and architecture of photosynthetic membranes of *R. photometricum* change in response to light. Despite large modifications in the membrane composition, the local environment of core complexes remained unaltered, whereas specialized

paracrystalline light-harvesting antenna domains grew under low-light conditions. It was concluded that such structural adaptation ensures efficient photon capture under low-light conditions and prevents photodamage under high-light conditions.

Live Cells

Progress in applying AFM imaging to microbial cells have been slower due essentially to difficulties associated with sample preparation and imaging conditions. While isolated membranes are generally well-immobilized by simple adsorption on mica [27], stronger attachment is often needed for whole cells [28]. This can be achieved by drying the sample or by bonding the cells covalently to the support. However, these treatments may cause significant rearrangement, denaturation or contamination of the cell walls, yielding information that may no longer be representative of the native state. More appropriate approaches include treating the support with a polycation to strengthen cell adhesion or immobilizing the cells mechanically in an agar gel or in a porous membrane. In the agar method, the gel is used as a soft, deformable immobilization matrix, thereby allowing direct visualization of growth processes [29]. In the porous membrane method, spherical cells are trapped in a polymer membrane with a pore size comparable to the dimensions of the cell, allowing repeated imaging in buffer solutions without cell detachment or cell damage [30].

Despite these technical difficulties, AFM is being used increasingly to visualize ultrastructural details on hydrated cells. *Saccharomyces cerevisiae* [31], *Phanerochaete chrysosporium* [32], *Aspergillus oryzae* [33], *Aspergillus nidulans* [34], *Pinnularia viridis* [35], lactic acid bacteria [36], *Bacillus* spores [37], *Staphylococcus aureus* [38], and *Mycobacterium bovis* [39, 40] are just a few examples of microbial species that have been explored by AFM in recent years.

Importantly, real-time imaging of live cells is revolutionizing our views of cell surface dynamics. High-resolution imaging of fungal spores has revealed dramatic changes of surface architecture during germination [33]. Figure 1 shows in situ, high-resolution images of *Aspergillus fumigatus* spores. The surface of dormant spores was covered with a crystalline-like array of rodlets, 10 nm in diameter, thought to play different biological functions such as spore dissemination and protection (Fig. 1a). In contrast, dramatic changes of cell surface structure occurred upon germination, the rodlet layer changing into a layer of amorphous material (Fig. 1b). Interestingly, a similar amorphous morphology, devoid of nanostructures, was observed for a mutant affected in rodlet formation (Fig. 1c), illustrating the usefulness of the technique in genetic mutation studies.

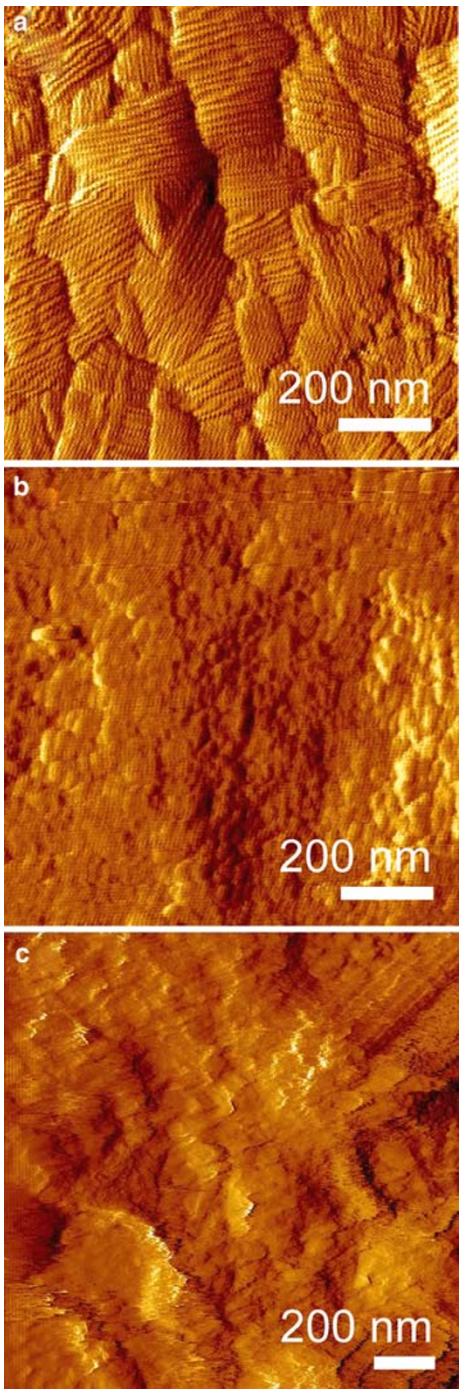

Fig. 1 Nanoscale imaging of live cells. (**a**) AFM deflection image in aqueous solution revealing rodlets on the surface of an *Aspergillus fumigatus* spore. (**b**) Image recorded on the same spore after 3 h germination, indicating that the crystalline rodlet layer has disappeared, revealing the underlying amorphous polysaccharide cell wall. (**c**) Image obtained for an *A. fumigatus* mutant deficient in rodlet production showing similar morphology as in **b**

Along the same line, cell growth and division events in *S. aureus* were monitored using AFM combined with thin-section TEM [38]. Nanoscale holes were seen around the

septal annulus at the onset of division and attributed to cell wall structures possessing high-autolytic activity. After cell separation, concentric rings were observed on the surface of the new cell wall and suggested to reflect newly formed peptidoglycan.

Of particular interest in biomedicine is the possibility to directly visualize the effect of drugs on cell surfaces. Early investigations performed in air demonstrated the ability of AFM to visualize drug-induced alterations in the cell walls of *E. coli* [41] *Helicobacter pylori* [42], and *S. aureus* [43]. More recently, drug-induced alterations were demonstrated on hydrated mycobacteria [40]. AFM imaging combined with quantitative roughness analysis was used to investigate the influence of three drugs (isoniazid, ethambutol, and streptomycine) on the surface of *M. bovis* BCG (Fig. 2). All the drugs tested induced an increase of surface roughness, to an extent correlated with the localization and specificity of the target. While native cells (Fig. 2a) showed homogeneous surfaces with very low roughness (0.5 nm on 500×500 nm^2 areas), cells treated with isoniazid and ethambutol were significantly rougher (1, 3 nm) (Fig. 2b, c). These effects were consistent with the action modes of the drugs, i.e., inhibition of mycolic acid and arabinogalactan synthesis, respectively. Streptomycine, that inhibits protein synthesis in general, thus not only in the cell wall, caused the largest increase in surface roughness (4 nm) (Fig. 2d). In the future, these non-invasive investigations may help understanding the action mode of antibiotics as well as the mechanisms of cell wall assembly.

Single Molecule Measurements

Molecular recognition between receptors and cognate ligands plays a central role in cellular behaviors. For instance, cell adhesion and aggregation is usually mediated through specific cell adhesion proteins such as lectins and adhesins. Using single molecule force spectroscopy, the molecular forces driving receptor–ligand interactions can be directly measured on live cells. Further, affinity imaging offers a means to localize specific molecules on cells, such as cell adhesion proteins and antibiotic binding sites [11, 44].

Molecular Recognition Forces

Molecular recognition studies with the AFM implies functionalizing the tips (and solid surfaces) with relevant biomolecules, using procedures that meet the following requirements [11, 44]: (a) the forces which immobilize the molecules should be stronger than the intermolecular force being studied; (b) the attached biomolecules should have enough mobility so that they can freely interact with complementary molecules; (c) the contribution of non-specific adhesion to the measured forces should be minimized; (d) attaching biomolecules at low surface density is

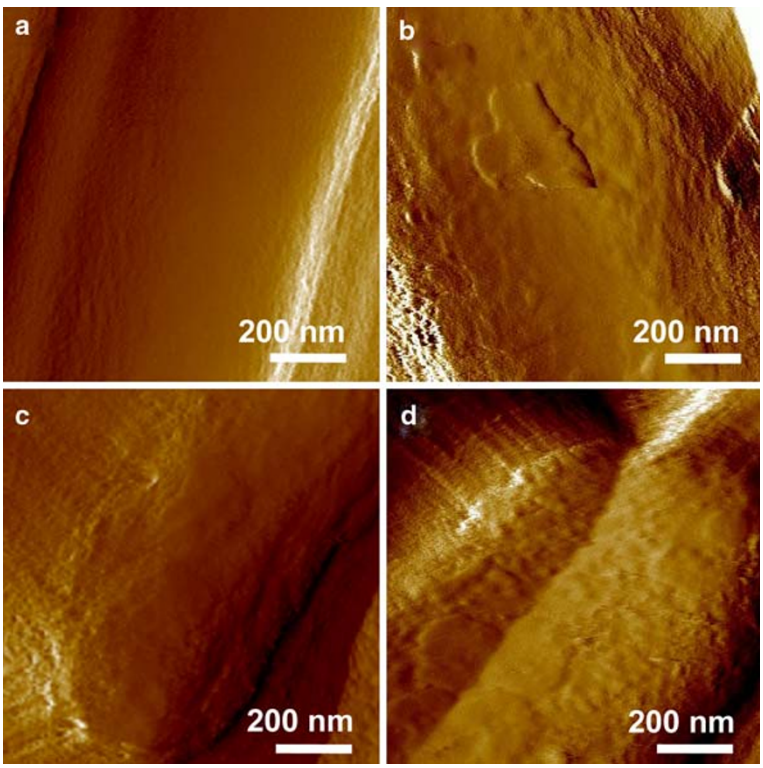

Fig. 2 Imaging bacteria following treatment with antibiotics. AFM deflection images in aqueous solution of *M. bovis* BCG cells, prior (**a**) and after treatment during 24 h with isoniazid (**b**), ethambutol (**c**), and streptomycine (**d**) at the minimum inhibitory concentration. All the drugs induced substantial modifications of the cell surface architecture, to an extent related to the specificity of the target

recommended in order to ensure single molecule detection; (e) site-directed coupling may be desired to orientate all the interacting molecules in the same way.

Molecular recognition forces are measured by recording force curves between modified tips and sample and then assessing the unbinding force between complementary receptor and ligand molecules from the adhesion force observed upon retraction. The measured unbinding forces are typically in the 50–400 pN range, depending on the experimental conditions [45–56]. Control experiments should always be carried out to demonstrate the specificity of the measured unbinding forces, which is best achieved by block experiments in which the receptor sites are masked by adding free ligands or by exploiting genetic mutation. Using these force spectroscopy experiments, a variety of ligand–receptor forces have been measured at the single molecule level including those associated with avidin/streptavidin [45, 46], antibodies [47], DNA [48], lectins [49], cadherins [50], integrins [51], and selectins [52]. The four later studies are particularly interesting in cellular biology since they concern the specific forces associated with cell adhesion proteins, thereby contributing to refine our understanding of cellular interactions.

The power of such single molecule analyses in microbiology is illustrated in Fig. 3 [39]. In bacterial pathogenesis, the infectious process is generally initiated by the interaction between adhesins on the bacterial cell surface and specific ligands on the host cell surface. *M. tuberculosis*, for instance, adheres to heparan sulphates on epithelial cells via a heparin-binding haemagglutinin adhesin (HBHA). To explore the unbinding forces of individual HBHA, force curves were recorded between HBHA-modified tips and heparin-coated supports (Fig. 3a). The adhesion force histogram obtained using a loading rate of 10,000 pN/s revealed a bimodal distribution with average rupture forces of 50 and 117 pN, attributed to one and two binding events between HBHA and heparin (Fig. 3b). The specificity of the measured interaction was confirmed by showing a dramatic reduction in the number of adhesion events when working in the presence of free heparin (Fig. 3c).

The mechanisms of action of drugs also rely on molecular recognition. For instance, the clinically important vancomycin antibiotic inhibits the growth of pathogens such as *S. aureus* by blocking cell wall synthesis through specific recognition of nascent peptidoglycan terminating

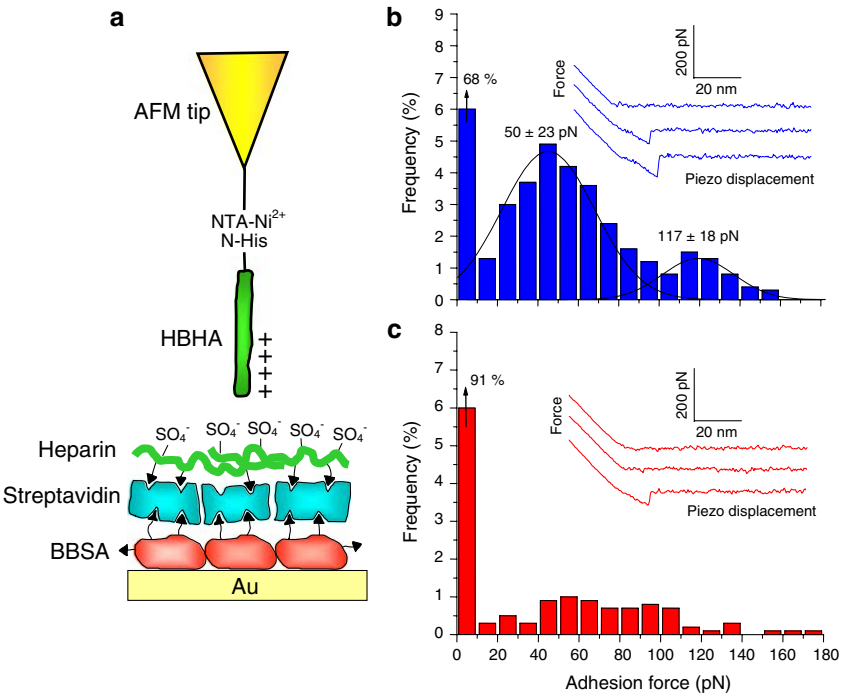

Fig. 3 Measuring the specific binding forces of individual adhesins. (**a**) Schematics of the surface chemistry used to functionalize the AFM tip and substrate with HBHA and heparin. Recombinant histidine-tagged HBHA were attached onto an AFM tip terminated with Ni^{++}-nitrilotriacetate (*NTA*) groups while biotinylated heparin was bound to a gold surface via streptavidin and biotinylated bovine serum albumin (*BBSA*) layers. (**b**) Representative force curves and adhesion force histogram obtained in PBS between a HBHA tip and a heparin surface. The adhesion force histogram revealed a bimodal distribution reflecting the binding strength of one and two adhesins. (**c**) Same experiment in the presence of free heparin (50 μg/ml) demonstrating a dramatic reduction of adhesion frequency due to the blocking of the HBHA adhesion sites. Reprinted with permission from ref. [39]

in D-Ala-D-Ala. Recently, the ability of AFM with vancomycin tips to measure the forces and the dynamics of the vancomycin/D-Ala-D-Ala interaction was demonstrated (Fig. 4; [53]). Gold tips and supports were functionalized with vancomycin and D-Ala-D-Ala-D-Ala peptides, respectively. Force-distance curves recorded between the modified surfaces displayed adhesion forces with a mean magnitude of 98 pN, that were attributed to the rupture of single vancomycin/D-Ala-D-Ala complexes. By varying the loading rate, i.e., the rate at which the force is applied to the bond, and the interaction time, it was possible to assess the association and dissociation rate constants. Accordingly, the above studies show that single-molecule force spectroscopy is a powerful tool to gain insight into molecular recognition events at cell surfaces.

Affinity Imaging

Notably, affinity imaging using adhesion force mapping provides unique possibilities for the identification and localization of specific receptors and ligands on cell surfaces. Here, arrays of force curves are recorded in the *x*, *y* plane on an area of given size, and the unbinding force values for all curves are assessed and displayed as gray pixels [54]. To date, this method has been applied to different cell types, including red blood cells [49], osteoclasts [55] and endothelial cells [56]. In microbiology, the approach was used to map the distribution of single HBHA adhesins on mycobacteria (Fig. 5, [39]). *M. bovis* BCG cells expressing HBHA were immobilized on a polycarbonate membrane, a method which allows live cells to be imaged without using any drying or fixation step (Fig. 5a). High-resolution images revealed a smooth and homogeneous surface (Fig. 5b), consistent with earlier scanning electron microscopy observations. Affinity maps (Fig. 5c, d) recorded on cells with a heparin-modified tip revealed adhesion events (bright pixels) in about half of the locations. The adhesion force magnitude was very close to the value expected for a single HBHA-heparin interaction, supporting the notion that single HBHA were detected. This was confirmed by showing that a mutant strain lacking HBHA did not bind the heparin tip. Interestingly, the HBHA distribution was not homogeneous, but apparently concentrated into nanodomains which may promote adhesion to target cells by inducing the recruitment of receptors within membrane rafts. In the future, these molecular recognition studies may help in the development of new drugs capable to block bacterial adhesion.

More recently, antibiotic-modified tips were used to map individual binding sites on live bacteria (Fig. 6, [53]). Fluorescent vancomycin was used to visualize D-Ala-D-Ala sites of nascent peptidoglycan in the cell wall of dividing *L. lactis* cells (Fig. 6a, b). Fluorescence staining of the wild-type strain was found around the septum, while no fluorescent labeling was detected for a mutant strain producing peptidoglycan precursors ending by D-Ala-D-Lac instead of D-Ala-D-Ala. AFM topographic images of *L. lactis* cells revealed a smooth and elongated cell morphology as well as a well-defined division septum (Fig. 6c). Ring-like structures were seen at a certain distance from the septum, presumably formed by an outgrowth of the cell wall. Notably, adhesion force maps demonstrated that binding sites were essentially located in the septum region, and more specifically on the equatorial rings (Fig. 6d), suggesting that newly formed peptidoglycan was inserted in these regions. This work shows that

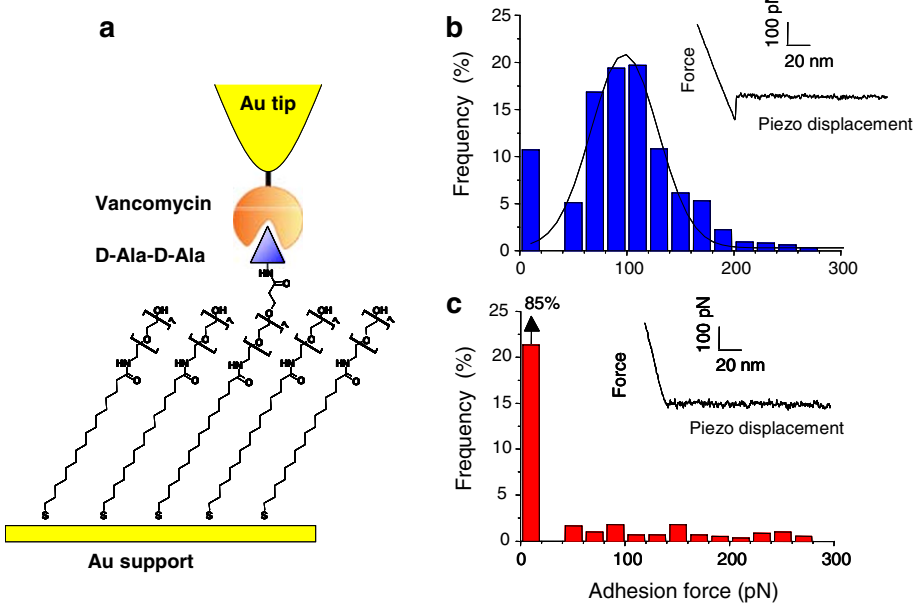

Fig. 4 Measuring the specific binding forces of antibiotics. (**a**) Gold tips were functionalized with bis(vancomycin) cystamide while gold supports terminated with propionic acid groups were covalently reacted with D-Ala-D-Ala-D-Ala peptides. (**b**) Representative force curve and adhesion force histogram obtained in PBS between a vancomycin tip and a D-Ala-D-Ala support. (**c**) Control experiment showing a dramatic reduction of adhesion frequency when the force measurements are performed in the presence of free D-Ala-D-Ala-D-Ala peptides. Reprinted with permission from ref. [53]

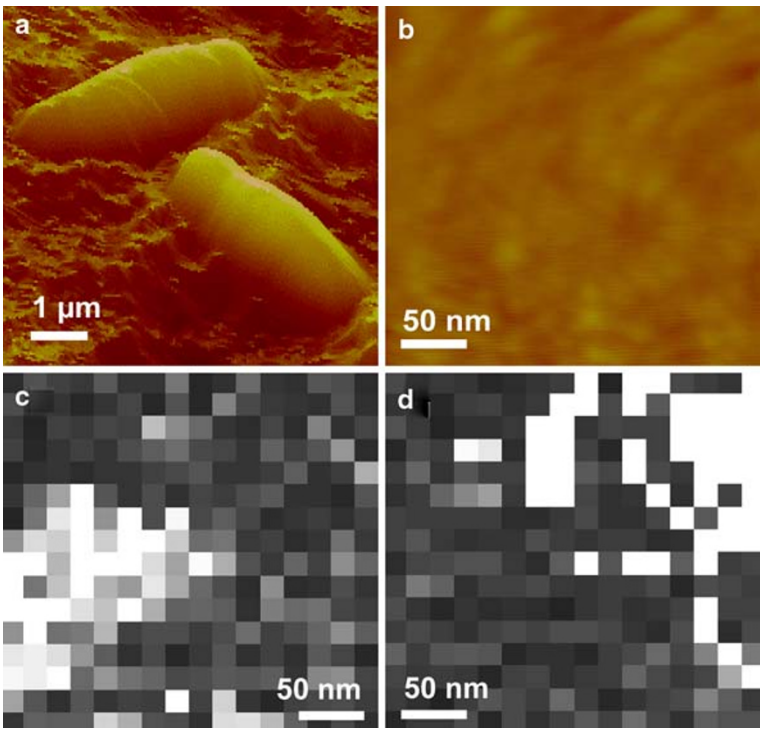

Fig. 5 Affinity imaging of cell surface adhesins. (**a**) AFM topographic image recorded in PBS showing two *M. bovis* BCG cells on a polymer substrate. (**b**) High-resolution image of the cell surface revealing a smooth morphology. (**c, d**) Two representative adhesion force maps (*gray* scale: 100 pN) recorded in PBS with a heparin-modified AFM tip. Adhesion events (*bright* pixels) reflect the detection of single adhesins. The adhesin distribution is not homogeneous, but apparently concentrated into nanodomains which may play important biological functions. Reprinted with permission from ref. [39]

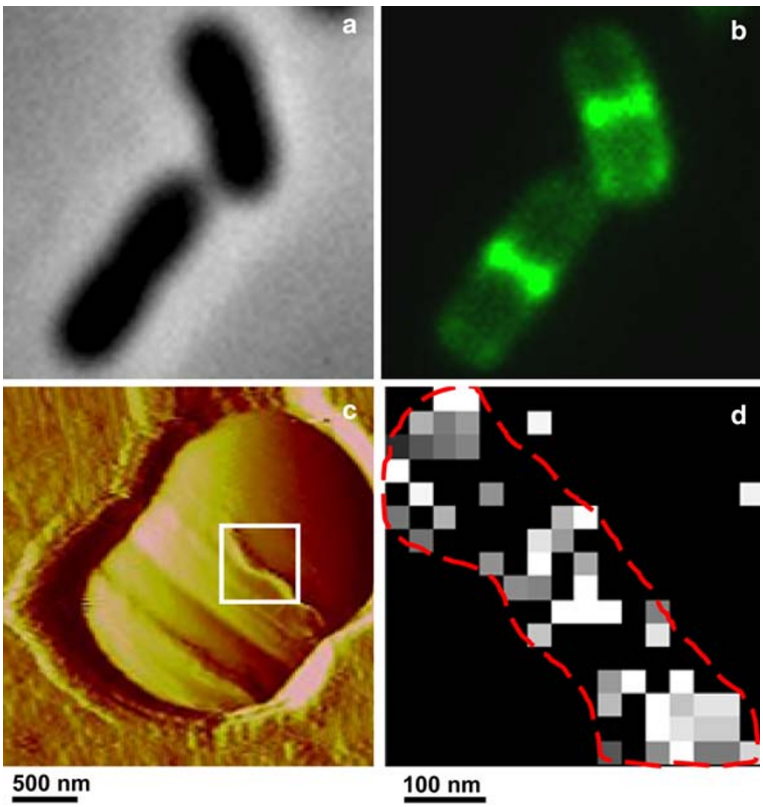

Fig. 6 Affinity imaging of antibiotic binding sites. (**a**) Phase contrast and (**b**) fluorescence image of *Lactococcus lactis* cells during the course of the division process. Fluorescent vancomycin accumulates at the division site, by attaching specifically to D-Ala-D-Ala sites of cell wall peptidoglycan. (**c**) AFM image of a cell showing a well-defined division septum as well as a ring-like structure expected to be rich in nascent peptidoglycan (*white box*). (**d**) Adhesion force map (*gray* scale: 100 pN) recorded with a vancomycin tip on the septum region (highlighted by the *white box* in **c**). Adhesion events are essentially located in the septum region (*red line*), more specifically on the ring-like structure, suggesting that newly formed peptidoglycan is inserted. Reprinted with permission from ref. [53]

AFM with vancomycin tips is a complementary approach to fluorescent vancomycin to explore the architecture and assembly process of peptidoglycan during the cell cycle of Gram-positive bacteria. While fluorescence microscopy generates microscale images allowing the localization of peptidoglycan in the entire cell wall, AFM reveals the distribution of single peptidoglycan molecules on the outermost cell surface.

Conclusions

This review shows that nanomicrobiology—the exploration of microbial cells on the nanoscale—is an exciting research field that has developed very rapidly in the past years. AFM imaging enables investigators to visualize, under physiological conditions, the surface structure of membranes and cell surfaces, with unprecedented resolution. Conformational changes of membrane proteins can be detected at subnanometer resolution in relation with function. Time-lapse imaging offers a means to follow dynamic events occurring at cell surfaces, such as cell growth and drug-induced alterations. Single molecule force spectroscopy allows researchers to measure the forces and dynamics of receptor–ligand interactions and to identify and localize specific sites on live cells. These nanoscale studies provide new avenues in many areas, particularly in biomedicine for investigating the mode of action of drugs, and for elucidating the molecular basis of host–pathogen interactions.

Acknowledgements This work was supported by the National Foundation for Scientific Research (FNRS), the Foundation for Training in Industrial and Agricultural Research (FRIA), the Région wallonne, the Université Catholique de Louvain (Fonds Spéciaux de Recherche), and the Federal Office for Scientific, Technical and Cultural Affairs (Interuniversity Poles of Attraction Programme). Y. F. D. is a Research Associate of the FNRS.

References

1. T.J. Beveridge, J. Bacteriol. **181**, 4725 (1999)
2. V.R.F. Matias, T.J. Beveridge, Mol. Microbiol. **56**, 240 (2005)
3. V.R.F. Matias, T.J. Beveridge, J. Bacteriol. **188**, 1011 (2006)
4. T.J. Beveridge, L.L. Graham, Microbiol. Rev. **55**, 684 (1991)
5. J. Ubbink, P. Schar-Zammaretti, Micron **36**, 293 (2005)
6. A. Engel, D.J. Müller, Nat. Struct. Biol. **7**, 715 (2000)
7. Y.F. Dufrêne, Nature Rev. Microbiol. **2**, 451 (2004)
8. D.J. Müller, K.T. Sapra, S. Scheuring, A. Kedrov, P.L. Frederix, D. Fotiadis, A. Engel, Curr. Opin. Struct. Biol. **16**, 489 (2006)
9. F. Gaboriaud, Y.F. Dufrêne, Colloids Surf. B Biointerfaces **54**, 10 (2007)
10. C.J. Wright, I. Armstrong, Surf. Interf. Anal. **38**, 1419 (2006)
11. P. Hinterdorfer, Y.F. Dufrêne, Nat. Methods **3**, 347 (2006)
12. H.J. Butt, B. Cappella, M. Kappl, Surf. Sci. Rep. **59**, 1 (2005)
13. E.S. Gyorvary, O. Stein, D. Pum, U.B. Sleytr, J. Microsc. **212**, 300 (2003)
14. D.J. Müller, W. Baumeister, A. Engel, J. Bacteriol. **178**, 3025 (1996)
15. D.J. Müller, F.A. Schabert, G. Büldt, A. Engel, Biophys. J. **68**, 1681 (1995)
16. F.A. Schabert, C. Henn, A. Engel, Science. **268**, 92 (1995)
17. D.J. Müller, A. Engel, J. Mol. Biol. **285**, 1347 (1999)
18. D.J. Müller, W. Baumeister, A. Engel, Proc. Natl. Acad. Sci. USA **96**, 13170 (1999)
19. F. Oesterhelt, D. Oesterhelt, M. Pfeiffer, A. Engel, H.E. Gaub, D.J. Müller, Science **288**, 143 (2000)
20. J.K. Hörber, J. Mosbacher, W. Häberle, J.P. Ruppersberg, B. Sakmann, Biophys. J. **68**, 1687 (1995)
21. R.P. Goncalves, G. Agnus, P. Sens, C. Houssin, B. Bartenlian, S. Scheuring, Nat. Methods **3**, 1007 (2006)
22. S. Scheuring, J. Seguin, S. Marco, D. Lévy, B. Robert, J.L. Rigaud, Proc. Natl. Acad. Sci. USA **100**, 1690 (2003)
23. S. Scheuring, J.N. Sturgis, Science **309**, 484 (2005)
24. S. Bahatyrova, R.N. Frese, C.A. Siebert, J.D. Olsen, K.O. van der Werf, R. van Grondelle, R.A. Niederman, P.A. Bullough, C. Otto, C.N. Hunter, Nature **430**, 1058 (2004)
25. S. Scheuring, J. Busselez, D. Lévy, J. Biol. Chem. **180**, 1426 (2005)
26. S. Scheuring, R.P. Goncalves, V. Prima, J.N. Sturgis, J. Mol. Biol. **358**, 83 (2006)
27. D.J. Müller, M. Amrein, A. Engel, J. Struct. Biol. **119**, 172 (1997)
28. K. El Kirat, I. Burton, V. Dupres, Y.F. Dufrene, J. Microsc. **218**, 199 (2005)
29. M. Gad, A. Ikai, Biophys. J. **69**, 2226 (1995)
30. S. Kasas, A. Ikai, Biophys. J. **68**, 1678 (1995)
31. F. Ahimou, A. Touhami, Y.F. Dufrêne, Yeast. **20**, 25 (2003)
32. Y.F. Dufrêne, C.J.P. Boonaert, P.A. Gerin, M. Asther, P.G. Rouxhet, J. Bacteriol. **181**, 5350 (1999)
33. B.C. van der Aa, R.M. Michel, M. Asther, M.T. Zamora, P.G. Rouxhet, Y.F. Dufrêne, Langmuir. **17**, 3116 (2001)
34. H. Ma, L.A. Snook, S.G.W. Kaminskyj, T.E.S. Dahms, Microbiol.-SGM **151**, 3679 (2005)
35. S.A. Crawford, M.J. Higgins, P. Mulvaney, R. Wetherbee, J. Phycol. **37**, 543 (2001)
36. P. Schar-Zammaretti, J. Ubbink, Biophys. J. **85**, 4076 (2003)
37. V.G.R. Chada, E.A. Sanstad, R. Wang, A. Driks, J. Bacteriol. **185**, 6255 (2003)
38. A. Touhami, M.H. Jericho, T.J. Beveridge, J. Bacteriol. **186**, 3286 (2004)
39. V. Dupres, F.D. Menozzi, C. Locht, B.H. Clare, N.L. Abbott, S. Cuenot, C. Bompard, D. Raze, Y.F. Dufrêne, Nat. Methods **2**, 515 (2005)
40. C. Verbelen, V. Dupres, F.D. Menozzi, D. Raze, A.R. Baulard, P. Hols, Y.F. Dufrêne, FEMS Microbiol. Lett. **264**, 192 (2006)
41. P.C. Braga, D. Ricci, Antimicrob. Agents Chemother. **42**, 18 (1998)
42. P.C. Braga, D. Ricci, Chemotherapy. **46**, 15 (2000)
43. S. Boyle-Vavra, J. Hahm, S.J. Sibener, R.S. Daum, Antimicrob. Agents Chemother. **44**, 3456 (2000)
44. V. Dupres, C. Verbelen, Y.F. Dufrêne, Biomaterials **28**, 2393 (2007)
45. G.U. Lee, D.A. Kidwell, R.J. Colton, Langmuir **10**, 354 (1994)
46. E.L. Florin, V.T. Moy, H.E. Gaub, Science **264**, 415 (1994)
47. P. Hinterdorfer, W. Baumgartner, H.J. Gruber, K. Schilcher, H. Schindler, Proc. Natl. Acad. Sci. USA **93**, 3477 (1996)
48. G.U Lee, L.A. Chrisey, R.J. Colton, Science **266**, 771 (1994)
49. M. Grandbois, W. Dettmann, M. Benoit, H.E. Gaub, J. Histochem. Cytochem. **48**, 719 (2000)
50. W. Baumgartner, P. Hinterdorfer, W. Ness, A. Raab, D. Vestweber, H. Schindler, D. Drenckhahn, Proc. Natl. Acad. Sci. USA. **97**, 4005 (2000)
51. X. Zhang, E. Wojcikiewicz, V.T. Moy, Biophys. J. **83**, 2270 (2002)
52. X. Zhang, D.F. Bogorin, V.T. Moy, Chem. Phys. Chem. **5**, 175 (2004)
53. Y. Gilbert, M. Deghorain, L. Wang, B. Xu, P.D. Pollheimer, H.J. Gruber, J. Errington, B. Hallet, X. Haulot, C. Verbelen, P. Hols, Y.F. Dufrêne, Nanolett. **7**, 796 (2007)
54. M. Ludwig, W. Dettmann, H.E. Gaub, Biophys. J. **72**, 445 (1997)
55. P.P. Lehenkari, G.T. Charras, A. Nykänen, M.A. Horton, Ultramicroscopy **82**, 289 (2000)
56. N. Almqvist, R. Bhatia, G. Primbs, N. Desai, S. Banerjee, R. Lal, Biophys. J. **86**, 1753 (2004)